

## MICROSTRUCTURE IN MIXED-LAYER ILLITE/SMECTITE AND ITS RELATIONSHIP TO THE REACTION OF SMECTITE TO ILLITE

T. E. BELL

Utah International Inc., 550 California Street, San Francisco, California 94104

**Abstract**—The reaction of smectite to illite in shale from the COST 1 well in the south Texas Gulf Coast and from altered ash-fall tuffs from the Morrison Formation in New Mexico was investigated using X-ray powder diffraction in conjunction with transmission electron microscopy. In the COST 1 well, the bulk of the detrital clay was originally a K<sup>+</sup>-deficient mixed-layer illite/smectite (I/S). As the I/S adsorbed K<sup>+</sup> released by the dissolution of K-feldspar during burial, the proportion of expandable layers decreased with depth from ~65% near the top of the well to ~25% at 4500 m depth. In contrast, the proportion of low-charged structural planes [ $<0.8$  eq per (Al,Si)<sub>4</sub>O<sub>10</sub> unit] in the I/S decreased gradually from ~40% near the top of the well to ~15% near the bottom. Authigenic smectite with 100% expandable layers from the Morrison Formation tuffs is an alteration product of vitric ash. Where these tuffs have been buried to ~1400 m the smectite has reacted to form I/S with ~15% expandable layers.

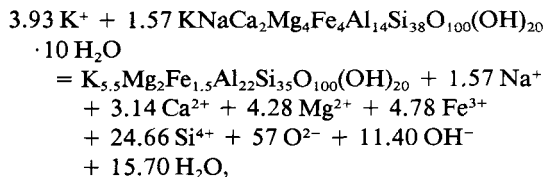
Direct lattice images of I/S crystallites from both locations reveal a correspondence between edge dislocations and the interface between illite layers and smectite layers. Al, Si, Fe, Ca, Mg, and Na were apparently mobile along these dislocations as the reaction of smectite to illite proceeded. Al was probably retained within the crystallite when illite layers replaced the smectite layers; however, some of the remaining cations were expelled. Lateral replacement of smectite layers by illite appears to have been the principal growth mechanism.

**Key Words**—Edge dislocation, Illite, Lattice image, Mixed layer, Smectite, Transmission electron microscopy, X-ray powder diffraction.

### INTRODUCTION

The exact mechanism by which smectite reacts to form illite during burial diagenesis or hydrothermal alteration is imperfectly understood. The range of geologic environments where this reaction is quantitatively important and the implications for interpreting environmental conditions of temperature and fluid composition are impetus for clarification of these reaction mechanisms. Burst (1959) suggested that smectite passes through an intermediate phase composed of coherent intergrowths of smectite and illite now called mixed-layer illite/smectite (I/S).

Much of our current understanding of this reaction stems from studies of burial diagenesis in the Texas Gulf Coast (Burst, 1969; Perry and Hower, 1970; Hower *et al.*, 1976; Boles and Franks, 1979). Hower *et al.* (1976) and Boles and Franks (1979) showed that the proportion of expandable (smectite) layers in I/S declines with depth in the Texas Gulf Coast. Hower *et al.* (1976) attributed this decrease to the reaction of smectite + K-feldspar to form quartz + illite with a loss of Fe and Mg from the smectite layers. Boles and Franks (1979) favored the reaction:



which implies that smectite layers provide the Al for the formation of illite.

X-ray powder diffractograms of I/S are thought to be generated by coherent intergrowths of illite and smectite (Reynolds and Hower, 1970; Reynolds, 1980). Recently, Nadeau *et al.* (1984a, 1984b) disputed this view based on X-ray powder diffraction (XRD) and transmission electron microscope (TEM) studies of natural smectite, illite, mixed-layer clays, and various physical mixtures of these clays. They showed that some apparent interstratification of illite and smectite is the result of interparticle X-ray diffraction. Their measurements of crystallite thickness from transmission electron micrographs suggested to them that smectite and illite occurred as discrete elementary particles 1–3 unit cells thick parallel to the *c* axis (Nadeau *et al.*, 1984a). They also suggested that, with burial, discrete elementary illite crystallites grew at the expense of elementary smectite crystallites, and the apparent increase in the proportion of illite layers in I/S was a result of interparticle diffraction among increasingly coarser elementary illite particles (Nadeau *et al.*, 1984b).

This present study addresses the nature of I/S by integrating XRD data with low- and high-magnification TEM images of crystallites from a cooperative stratigraphic test well (COST 1) in the Texas Gulf Coast and from altered ash-fall tuffs in the Morrison Formation, San Juan basin, New Mexico. XRD was used to determine the proportion of expandable layers in I/S before and after saturation with K<sup>+</sup>. Microstructure

and its relationship to the reaction of smectite to illite was investigated by TEM.

### GEOLOGIC SETTING

The COST 1 well penetrated 4870 m of Miocene to Recent sediments east of South Padre Island (96°40'W, 26°25'N). Shale and mudstone constitute the majority of the section with thin limestone and siltstone stringers occurring locally. Much of the section is undercompacted, and a geopressed zone exists between 2900 and 3810 m. The thermal gradient above 2800 m is 2.95°C/100 m and 3.22°C/100 m below 2800 m. The temperature at 2750 m is about 100°C, and the bottom-hole temperature is 172.5°C. Detrital minerals include I/S, quartz, plagioclase, K-feldspar, muscovite, biotite, hornblende, unidentified altered mafic minerals, and calcite. The clay mineralogy of samples from the COST 1 well consists primarily of I/S with minor amounts of chlorite and kaolinite.

Four samples of authigenic smectite, collected from outcrops of altered ash-fall tuffs of the Morrison Formation (upper Jurassic) in New Mexico, and I/S from drill core that intersected the same tuffs at depth were also examined. Outcrop samples were collected at Poison Canyon near Grants, New Mexico, and the drill core came from the CC-4 bore hole near Chaco Canyon National Monument, New Mexico. Smectite from outcropping tuffs is composed of 100% expandable layers, whereas their equivalents, buried to ~1400 m, are composed of I/S with ~15% expandable layers (Bell, 1986).

### EXPERIMENTAL TECHNIQUES

#### *Sample preparation and X-ray powder diffraction examination*

Drill cuttings from the COST 1 well were sampled at about 150-m intervals starting at 840 m and ending at 4500 m depth. The cuttings were washed and then soaked overnight in distilled water. Following gentle hand disaggregation, clay-water suspensions were prepared with distilled water from which the <0.5- $\mu$ m size fraction was isolated. Three splits were made of each sample. One split was mounted on frosted glass slides following the methods of Drever (1973). These clay mounts were warmed in an oven at 60°C and then sprayed with ethylene glycol from an atomizer. The sprayed samples were stored overnight in a desiccator over ethylene glycol at 60°C. The following day, each clay mount was scanned at 2°2 $\theta$ /min from 3° to 50°2 $\theta$  with Ni-filtered CuK $\alpha$  radiation on a Philips diffractometer. The proportion of expandable layers was estimated using the method of Reynolds and Hower (1970).

A second split was treated with a 3 N aqueous KCl solution at 60°C for 24 hr, washed repeatedly with distilled water, and dialyzed until all excess salts were

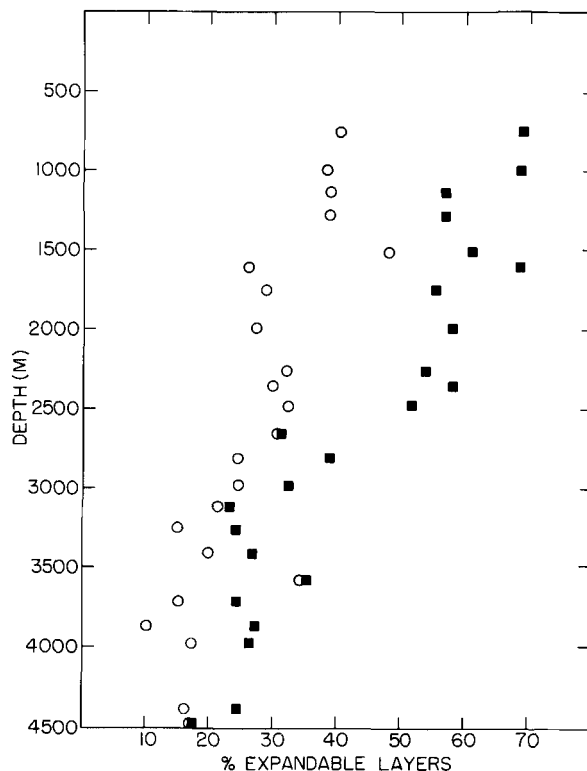


Figure 1. Plot of the proportion of expandable layers vs. burial depth in I/S from the COST 1 well. Solid squares are untreated, open circles are K<sup>+</sup>-saturated samples.

removed. The samples were then mounted on glass slides, glycolated, and X-rayed; the proportion of expandable layers was estimated as above.

#### *Transmission electron microscopy*

A third split was examined at 300 m intervals by TEM. Initial preparation of all TEM samples, including those from the Morrison Formation, involved exchange of n-alkylamine ions for the natural population of inorganic ions in interlayer sites. Ion exchange was accomplished by treating the <0.5- $\mu$ m size fraction with an aqueous 0.1 N dodecylamine HCl solution at 60°C for 10 days. Excess salts were removed by repeated washings with anhydrous methanol. The clay was further treated by suspending it in an identical dodecylamine solution at 60°C for 48 hr, followed by repeated washings as before to remove excess amine.

Treated samples were mounted for use in the TEM using a modified version of the procedure described by Lee *et al.* (1975) in which a slurry of treated clay and methanol was pipeted into flat molds half full of cured Spurr Low-Viscosity embedding medium. The methanol and remaining water were removed by evaporation in a vacuum for 3–5 days leaving the dehydrated clay crystallites in a preferred orientation. The molds were filled to the top with the remaining resin

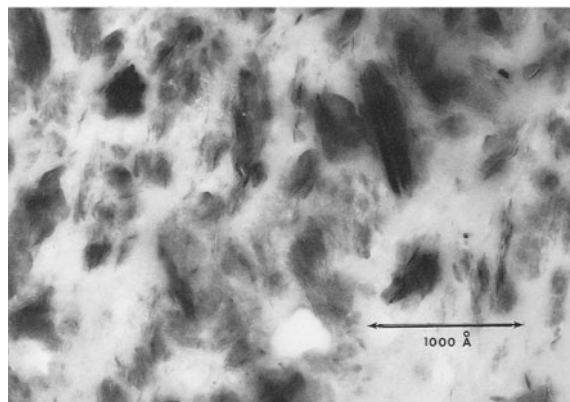


Figure 2. Low-magnification transmission electron micrograph of oriented I/S crystallites from the COST 1 well, 2050 m depth.

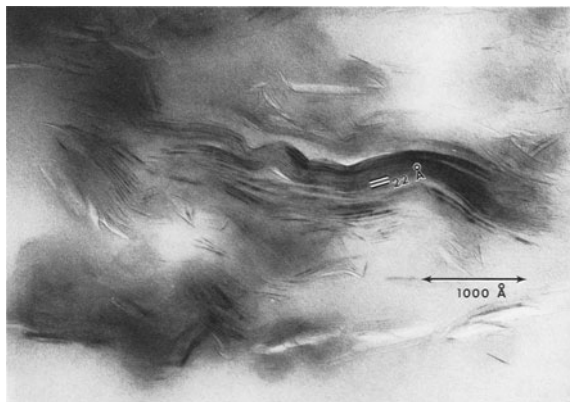


Figure 3. Direct lattice image of a folded, dodecylamine-saturated, clay crystallite from the COST 1 well, 2050 m depth.

and cured for 8 hr at 60°C in a partial vacuum. The molded epoxy-clay “sandwiches” were embedded in Beem capsules with more epoxy and cured for an additional 24–72 hr until the epoxy had the desired hardness. Cured samples were trimmed to the shape of a truncated pyramid ~0.5 mm on a side with a Porter-Blum MT-2 microtome. Ultra-thin sections (500–1000 Å thick) were sliced normal to the (001) crystallographic plane on the microtome and subsequently collected and mounted on Formvar-coated, copper TEM grids. Finally, a thin coat of carbon was applied to the mounts in a vacuum evaporator.

Prepared samples were viewed with a JEOL 100c transmission electron microscope at an accelerating voltage of 100 kV. High-magnification micrographs of COST 1 and Morrison samples were made of individual crystallites to determine the distribution of layer charge in the clay structure and the distribution of crystal defects.

## RESULTS

### *X-ray powder diffraction*

The unsaturated sample split was examined to determine the natural population of expandable layers in I/S from the COST 1 well. The proportion of expandable layers decreased from ~65% to ~25% over the stratigraphic interval sampled (Figure 1). Most of the decrease occurred in the interval from 2440 to 3050 m.

The purpose of K<sup>+</sup> saturation was to determine the proportion of high [ $>0.8$  eq per (Al,Si)<sub>4</sub>O<sub>10</sub> unit] to low-charge [ $<0.8$  eq per (Al,Si)<sub>4</sub>O<sub>10</sub> unit] layers. Layer charge arises from substitution of Al<sup>3+</sup> for Si<sup>4+</sup> in tetrahedral sites and/or from Me<sup>2+</sup> substitution for Me<sup>3+</sup> in octahedral sites, and is balanced by the charge of the ions in the interlayer sites. High-charge layers are capable of irreversibly dehydrating K<sup>+</sup> and, when K<sup>+</sup>-saturated, are not expandable with ethylene glycol

(Howard, 1981). They include illite layers, illite layers that have acquired hydrated cations in exchange for K<sup>+</sup> during weathering without a loss in layer charge, or smectite layers that have undergone an increase in layer charge during burial without having exchanged K<sup>+</sup> for the hydrated cations in interlayer sites.

Following K<sup>+</sup> saturation, the proportion of expandable layers decreased relative to the same unsaturated material for all samples (Figure 1), indicating a significant proportion of the layers had a high enough charge to dehydrate the K<sup>+</sup>, rendering them non-expandable. The most dramatic decreases in expandability between K<sup>+</sup>-saturated and unsaturated splits of the same sample occurred at  $>2740$  m. The proportion of expandable layers in the K<sup>+</sup>-saturated split also decreased with depth from ~40% to ~15% over the entire stratigraphic interval. In contrast to the unsaturated material, which showed its largest decrease over a 600-m interval, the proportion of expandable layers in the K<sup>+</sup>-saturated I/S decreased more uniformly with depth.

### *Transmission electron microscopy*

Low-magnification electron micrographs illustrate the range of crystallite sizes found in samples from the COST 1 well (Figure 2). The smallest crystallites are only a few unit cells thick parallel to the *c* axis and comprise a significant portion of samples from all depths. Many crystallites contain coherent zones 200 Å thick parallel to the *c* axis. Some of these thicker crystallites are aggregates of thinner crystallites analogous to the elementary silicate particles reported by Nadeau *et al.* (1984a). Others, however, are similar to the larger crystallites shown in transmission electron micrographs of *in situ* smectite and I/S by Page and Wenk (1979), I/S by Ahn and Peacor (1984), and illite by Eggleton and Buseck (1980). The similarity suggests that many of the crystallites from the COST 1 well are

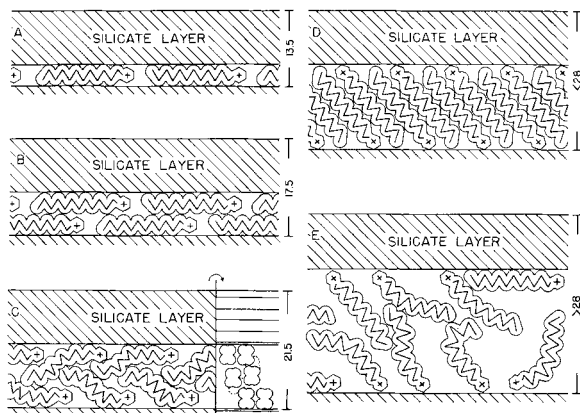


Figure 4. Configuration of dodecylamine ions in crystallites with different layer charges. (a) monolayer in low-charge montmorillonite,  $d(001) = 13.5 \text{ \AA}$ ; (b) bilayer in high-charge montmorillonite,  $d(001) = 17.5 \text{ \AA}$ ; (c) pseudotrimerolecular layer in very high-charge montmorillonite,  $d(001) = 21.5 \text{ \AA}$ ; (d) paraffin-like layer in illite,  $d(001) = 18\text{--}28 \text{ \AA}$ ; (e) non-equilibrium layer,  $d(001) > 28 \text{ \AA}$ . Modified from Lagaly and Weiss (1969) and Lagaly (1982).

not aggregates but single, albeit imperfect, clay crystallites.

High-resolution TEM indicates that individual crystallites of I/S have a highly irregular structure (Figures 2 and 3). The internal texture of individual crystallites from the COST 1 well is turbostratic, i.e., lattice planes or small clusters of planes are not parallel to their neighbors, but curved and twisted in a felt-like configuration. In addition, compaction has resulted in kinked and complexly folded crystallites. As a result, the domains which can coherently scatter X-rays are on the order of a few tens of  $d(001)$  planes thick and a few hundred Ångstrom units wide. These sizes are in approximate agreement with measurements made by Reynolds (1968) and are reflected by relatively low-intensity X-ray diffraction signals.

Saturation with dodecylamine prior to examination with the TEM allowed an estimation of the charge of individual layers. Close examination of almost any layer revealed a continuously variable spacing which was due to variations in the configuration of dodecylamine ions. The configuration of dodecylamine ions was in turn directly attributable to local variations in layer charge. Upon ion exchange with dodecylamine, low-charge smectite layers [ $<0.6$  eq per  $(\text{Al,Si})_4\text{O}_{10}$  unit] expanded to  $d(001)$  spacings of 13.5 or 17.5 Å (Figures 4a and 4b) (Lagaly and Weiss, 1969). High-charge smectites [ $0.6\text{--}0.8$  eq per  $(\text{Al,Si})_4\text{O}_{10}$  unit] expanded to 21.5 Å (Figure 4c) (Lagaly, 1982). Interpreting  $d(001)$  spacings greater than 21.5 Å is problematic. Lagaly (1982) attributed these larger spacings in high-charge vermiculite [ $>0.8$  eq per  $(\text{Al,Si})_4\text{O}_{10}$  unit] to arrangements of n-alkylamine ions into paraffin-like layers as

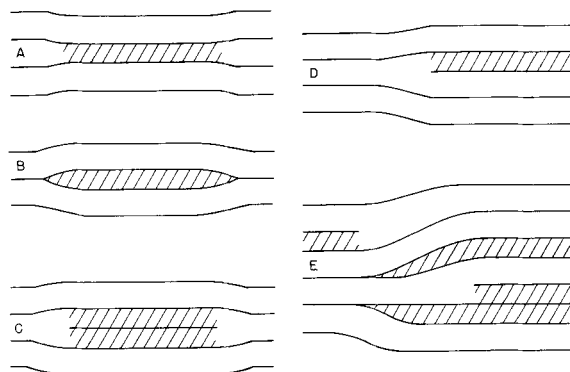


Figure 5. Types of interfaces between smectite layers (striped) and illite layers (open) after saturation with dodecylamine. (A) conservative boundary, i.e., no change in the number of lattice planes; (B) non-conservative boundary; bifurcating structural layers with a net loss in the number of lattice planes; (C) and (D) non-conservative boundaries; terminating structural layers with a net loss in the number of lattice planes. (E) combination of non-conservative boundaries, i.e., complex of edge dislocations where smectite layers are contributing components to growing illite layers.

depicted in Figure 4d. The spacing of these dodecylamine-saturated structures is dependent on the angle that the long axis of the ions makes with the silicate layer. As the layer charge increases, the number of ions per unit area increases to balance the charge, resulting in a greater angle between the long axis of the ions and the silicate layer. Thus, in theory, it is possible to estimate the approximate charge of individual layers or portions of layers by measuring their spacing on lattice images of crystallites. Layers with spacings of 22–28 Å were found to be common in crystallites from both the COST 1 well and the CC-4 borehole in New Mexico, and no layers were found with 10-Å spacings. These layers have been interpreted as illite layers, whose charge, as noted earlier, is  $>0.8$  eq per  $(\text{Al,Si})_4\text{O}_{10}$  unit.

Several patterns of I/S microstructure are common in the COST 1 and Morrison samples. As noted above, continuous variations in layer charge in adjacent and within individual layers are common, ranging from  $<0.6$  to 1.0 eq per  $(\text{Al,Si})_4\text{O}_{10}$  unit. Figure 5a schematically represents the most extreme variation in layer charge in which a smectite layer (striped) merges laterally with an illite layer (open). This texture results from direct conversion of the smectite layer which conserves the number of lattice planes. These conservative boundaries account for only a small portion of the illite layer-smectite layer interfaces and tend to be most abundant near the edge of crystallites. An example of this type of interface is shown in Figure 6 where a layer with 14-Å spacing (low-charge or smectite layer) expands to 25 Å (high-charge or illite layer) near the crystallite edge.

Crystal defects such as edge dislocations are common

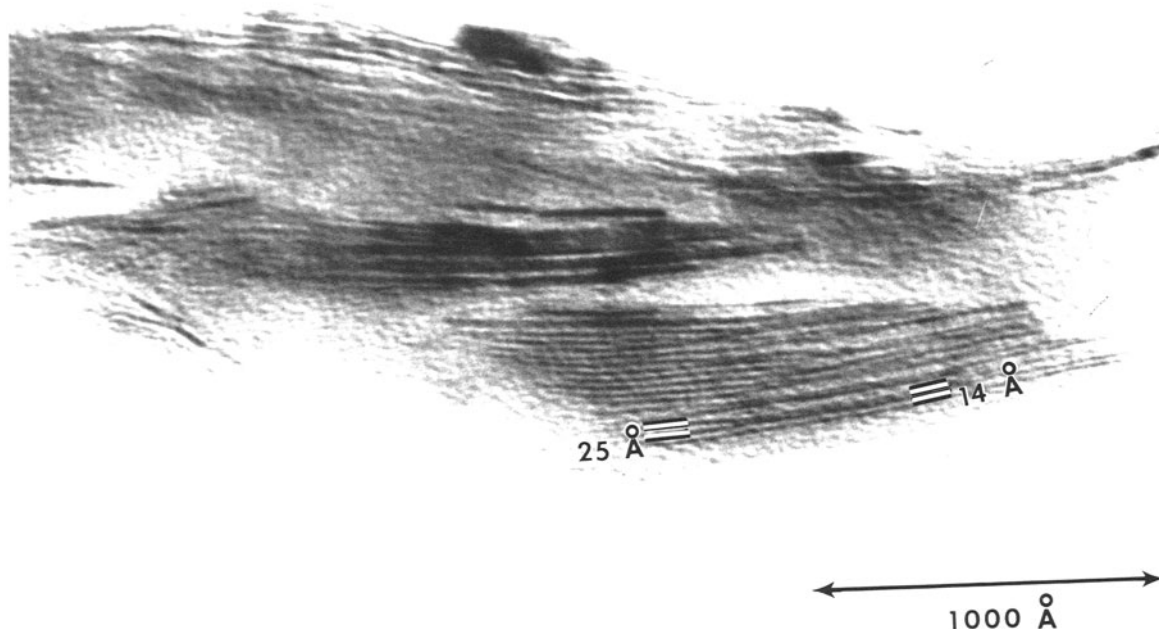


Figure 6. Direct lattice image of a dodecylamine-saturated I/S crystallite from the COST 1 well, 3970 m depth. Note that a smectite layer (14 Å) passes directly into an illite layer (25 Å), conserving the number of structural layers.

in I/S crystallites from the COST 1 well. Edge dislocations are non-conservative boundaries where terminating and bifurcating lattice planes of various types form the boundary between illite and smectite layers (Figure 7). Net losses in the number of lattice planes at the juncture of smectite and illite layers as shown in Figure 5b were common in all I/S crystallites and probably resulted from replacement of smectite by illite layers. Terminating lattice planes, such as those shown in Figures 5c and 5d, are also abundant, and consist of isolated smectite layers (striped) enclosed within illite layers (open). Figure 5e represents a typical combination of these different kinds of edge dislocations. The high density of edge dislocations in I/S and their association with the interface between illite layers and smectite layers suggests that they played an important role in the reaction of smectite to illite.

In contrast to the COST 1 samples, smectite crystallites from the Morrison Formation are many tens to hundreds of Ångstrom units thick, are less turbostratic, have much lower dislocation densities, and show little variation in layer charge within or between layers (Figure 8). Morrison Formation tuffs buried to a depth of 1400 m are composed of I/S which shows the same

correspondence of edge dislocations with illite-smectite boundaries common in I/S from the COST 1 well (Figure 9).

#### DISCUSSION

Howard (1981) suggested that the reaction of smectite to illite proceeded by two independent steps: an increase in layer charge by  $Al^{3+}$  substitution for  $Si^{4+}$  in tetrahedral sites, and a fixation and dehydration of  $K^+$  in interlayer sites. A comparison of  $K^+$ -saturated and untreated I/S demonstrates that the original 2:1 clay present in the COST 1 well was actually a  $K^+$ -deficient, illite-rich, I/S. No changes in the layer charge by tetrahedral substitution of  $Al^{3+}$  for  $Si^{4+}$  or exchange of  $Me^{2+}$  for  $Me^{3+}$  ions in octahedral sites were necessary for a major decrease in expandable layers if sufficient  $K^+$  had been available. As shown in Figure 1, as much as 30% reduction in the proportion of expandable layers resulted from  $K^+$  saturation, suggesting that the supply of  $K^+$  during burial was insufficient to replace the hydrated cations in illite layers.

The  $K^+$  available during burial was apparently derived from the dissolution of detrital K-feldspar. Scanning electron micrographs of K-feldspar grains show a

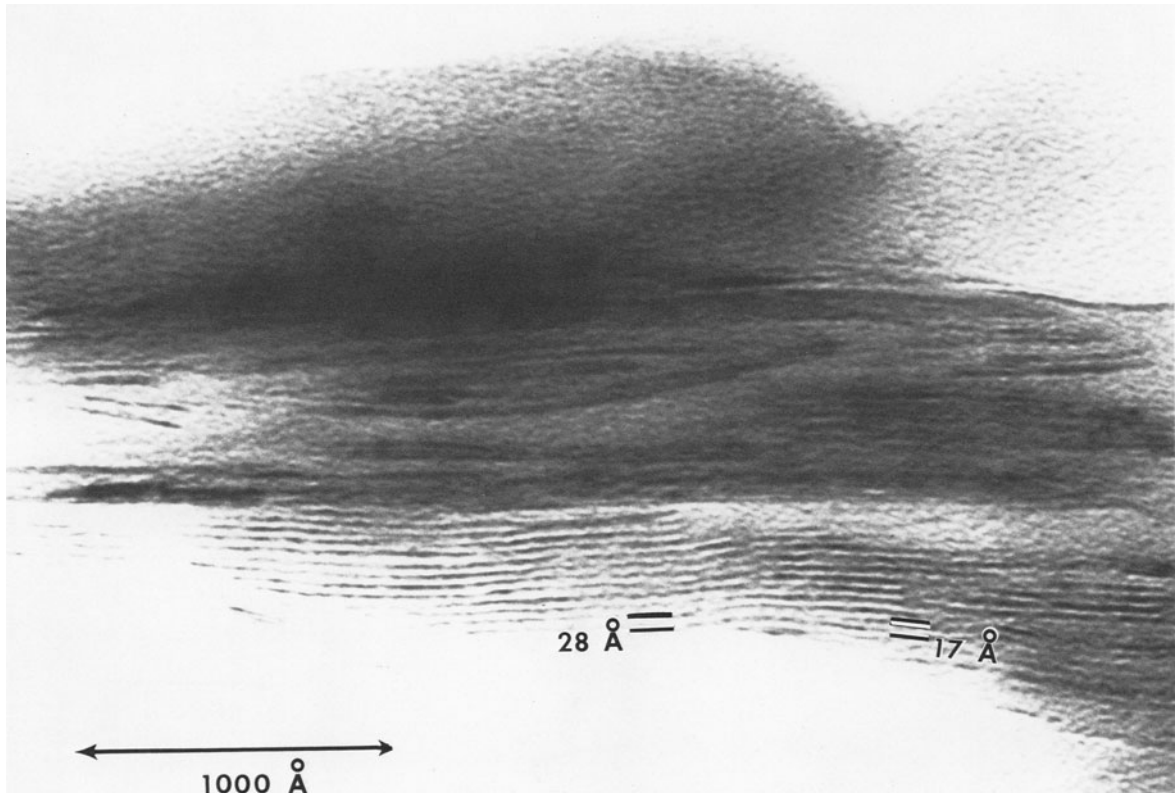


Figure 7. Direct lattice image of a dodecylamine-saturated, I/S crystallite from the COST 1 well, 3970 m depth. Note the termination of the upper structural layer in the smectite layer (17 Å) as it passes into an illite layer (28 Å).

progression of dissolution features with depth in the COST 1 well. Etch pits are visible on the surfaces of K-feldspar grains at 1800 m and become more prominent with depth. K-feldspar is absent below 3270 m, and the few grains remaining at this depth are deeply etched. K-feldspar grains are intensely etched and finally disappear over the same stratigraphic interval (1800–3270 m) in which the greatest reduction in expandable layers occurs (Figure 1). The high-charge layers in the I/S readily adsorbed  $K^+$  released by the dissolving K-feldspar. The efficiency of weathered illite to extract  $K^+$  from solution is well known (Sawhney, 1972).

The increase in layer charge was a much more gradual process as can be seen in Figure 1 where the proportion of expandable layers in the  $K^+$ -saturated split decreases from ~40% to ~15% over 3660 m of burial depth. Boles and Franks (1979) proposed that Al necessary for the reaction of smectite to illite was derived from the destruction of some smectite layers and the direct conversion of others. The abundance of edge dislocations at the interface between illite layers and smectite layers within crystallites is consistent with this

view. Despite an increase in layer charge, the new layers may still have behaved as smectite layers (expandable with ethylene glycol) unless they contained  $K^+$  in interlayer sites.

The association of edge dislocations with the boundary between illite and smectite along individual layers also suggests that much of the illite growth proceeded laterally. As the smectite structure was destroyed or altered, the illite structure grew in its place. As noted above, conservative boundaries, i.e., those with no visible destruction of the smectite structure (Figure 5a) are less common than non-conservative boundaries, i.e., those where terminating smectite layers form edge dislocations (Figures 5b–5e).

The trend of decreasing expandability with depth is complete by 3000 m leaving a residuum of 10–20% expandable layers which persists to the bottom of the COST 1 well (Figure 1). A similar trend was reported by Hower *et al.* (1976) and Boles and Franks (1979) for other Gulf Coast sections. Residual expandability may be the result of interparticle diffraction (Nadeau *et al.*, 1984a) or a failure of the smectite-illite reaction to go to completion. As noted above, a significant pro-

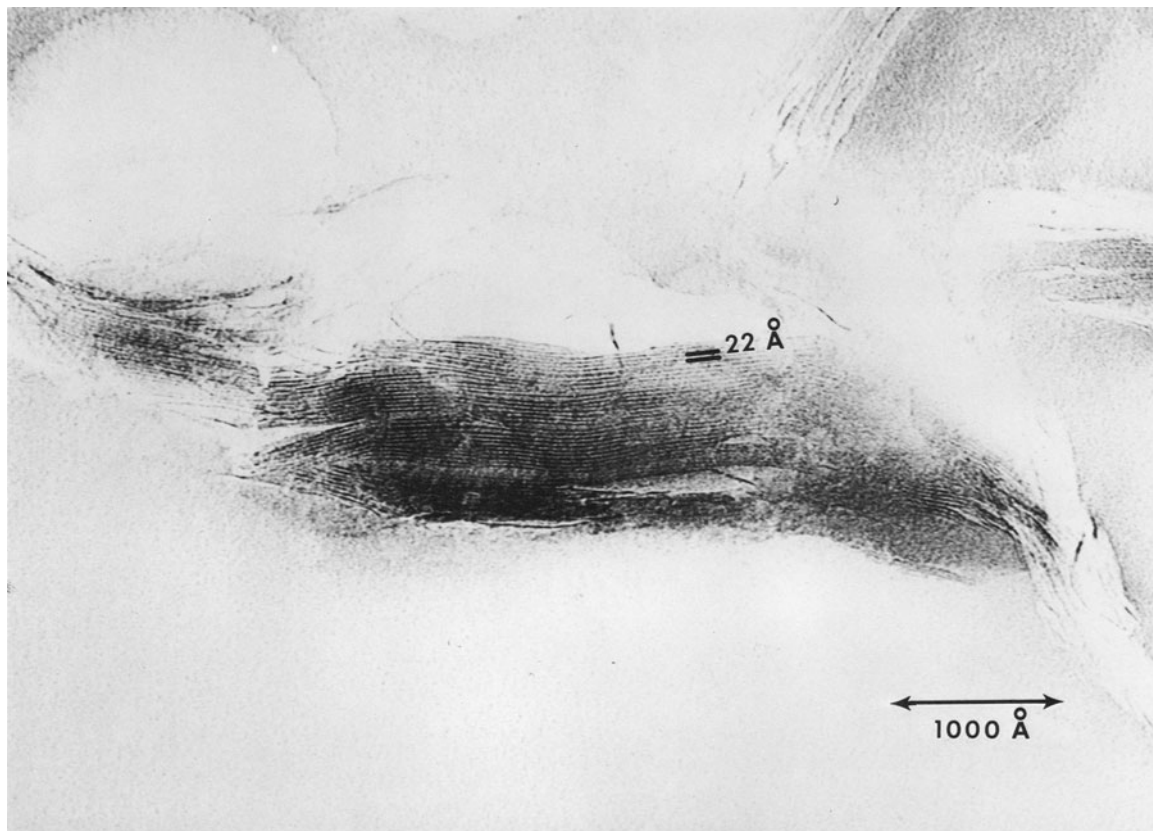


Figure 8. Direct lattice image of a dodecylamine-saturated smectite crystallite (22 Å), Morrison Formation outcrop. This crystallite has few edge dislocations or variations in layer charge either between or along layers.

portion of the I/S crystallites at all depths in the COST 1 well are only a few unit cells thick parallel to the  $c$  axis; therefore some of the apparent residual expandability could be due to interparticle diffraction. In the present study, no attempt was made to quantify the proportion of smectite layers from direct lattice images; it was noted, however, that below 3000 m crystallites with smectite layers are generally rare, although by no means absent (Figure 7). If interparticle diffraction accounts for 10% of the expandability over the entire depth of the COST 1 well, the true proportion of smectite layers is closer to 30% near the top of the well and decreases to ~5% at 3000 m depth, significantly lower values of expandability than have been reported in XRD studies of other sections in the Gulf Coast area (Hower *et al.*, 1976; Boles and Franks, 1979).

Weathering, transport, and compaction of the detrital I/S in samples from the COST 1 well have caused a degree of crystal damage and chemical alteration not seen in the authigenic smectite from the Morrison Formation. Despite these differences in starting material, the association of edge dislocations with the boundary

between illite layers and smectite layers is similar in the I/S from the COST 1 well and the buried Morrison tuffs. I/S from both locations has lateral transitions along individual layers from smectite to illite suggesting that this may be a common feature of I/S.

### CONCLUSIONS

The results of this study support the concept of interstratification of illite layers and smectite layers within individual crystallites as proposed by Reynolds and Hower (1970) and Reynolds (1980). In addition, the charge heterogeneity in 2:1 clays noted by Lagaly and Weiss (1969) and Lagaly (1982) was found to be common, not only in adjacent layers but within individual layers. The results differ from the recent work of Nadeau *et al.* (1984a and 1984b) in two respects: First, smectite crystallites from the Morrison Formation and many I/S crystallites from the COST 1 well are coherent over several to tens of unit cells along the  $c$  axis. Second, interstratification of illite and smectite within individual crystallites was found to be common.

Degraded I/S with a large proportion of high-charge

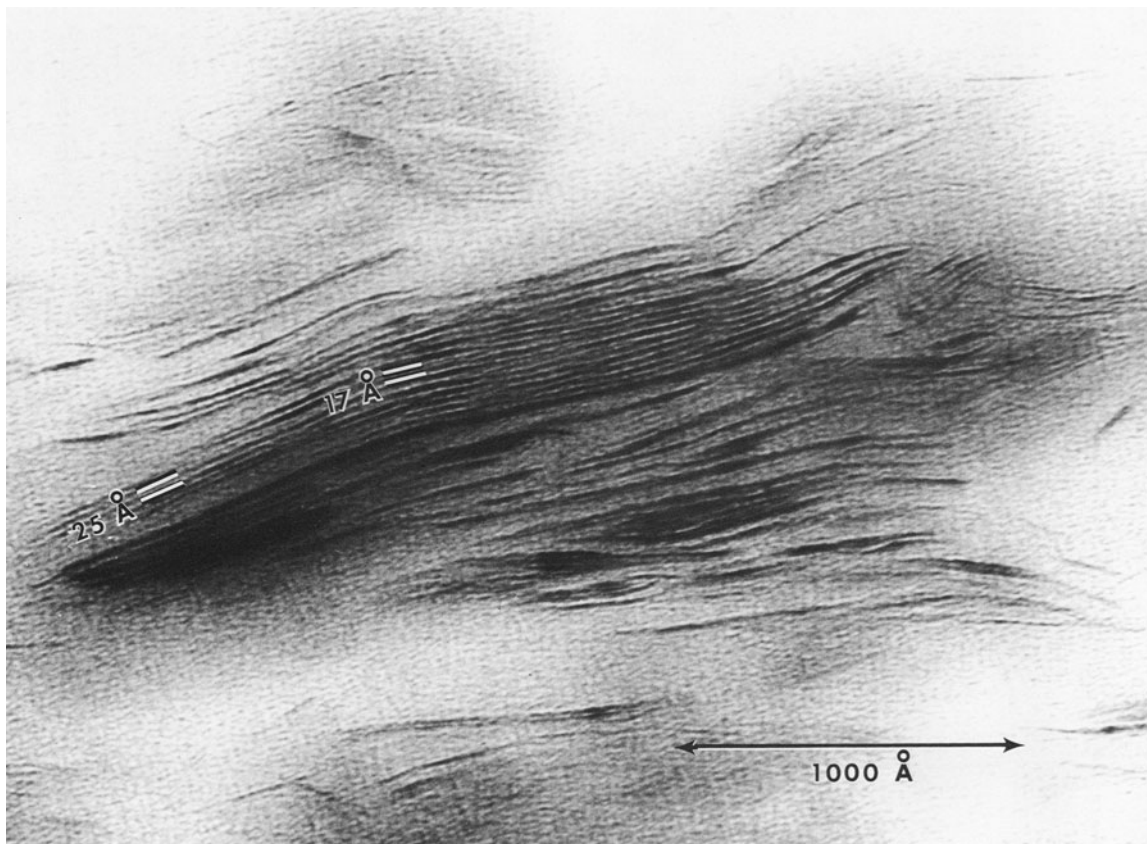


Figure 9. Direct lattice image of a dodecylamine-saturated I/S crystallite, Morrison Formation 1400 m burial depth. Bifurcating and terminating lattice planes are common between smectite layers (17 Å) and illite layers (25 Å).

layers was deposited at the site of the COST 1 well in the Texas Gulf Coast. Much of the decrease in expandability with depth was likely due to ion exchange of  $K^+$  for the metal ions acquired during weathering and transport rather than to an increase in layer charge. Ion exchange in I/S was apparently rapid, at least where the proportion of expandable layers was high and a ready supply of  $K^+$  was available. The increase in layer charge seems to have been much more gradual. The variation of charge along individual layers and the correspondence of edge dislocations with the boundaries between illite layers and smectite layers within crystallites point to internal utilization of the components common to both smectite and illite to form new illite layers.

#### ACKNOWLEDGMENTS

This study constitutes research done for ARCO Oil and Gas Company at their research center in Plano, Texas, and at the Department of Geology and Geophysics and the Electron Microscopy Laboratory of the University of California at Berkeley. I gratefully ac-

knowledge Dr. S. G. Franks and the staff at ARCO, Professor H. R. Wenk and Dr. J. Ainsworth at the Department of Geology and Geophysics, and C. Schooley at EML for their advice, criticism, and generosity during the course of this work.

#### REFERENCES

- Ahn, J. H. and Peacor, D. R. (1984) The TEM and AEM characterization of chlorite diagenesis in Gulf Coast argillaceous sediments: *Geol. Soc. Amer., Abstracts with Programs* **16**, p. 427.
- Bell, T. E. (1986) Depositional and diagenetic trends in the Brushy Basin and upper Westwater Canyon Members of the Morrison Formation, San Juan basin, New Mexico: in *A Basin Analysis Case Study: Uranium in the Morrison Formation, New Mexico*, C. E. Turner-Peterson and E. Santos, eds., Amer. Assoc. Petrol. Geol., Studies in Geology (in press).
- Boles, J. R. and Franks, S. G. (1979) Clay diagenesis in Wilcox sandstones of southwest Texas: implications of smectite diagenesis on sandstone cementation: *J. Sed. Petrol.* **49**, 55–70.
- Burst, J. F. (1959) Post-diagenetic clay mineral environmental relationships in the Gulf Coast Eocene: in *Clays and Clay Minerals, Proc. 6th Natl. Conf., Berkeley, California*,



- 1959, Ada Swineford, ed., Pergamon Press, New York, 327–341.
- Burst, J. F. (1969) Diagenesis of Gulf Coast clayey sediments and its possible relation to petroleum migration: *Amer. Assoc. Petrol. Geol. Bull.* **53**, 73–79.
- Drever, J. I. (1973) The preparation of oriented clay mineral specimens for X-ray diffraction analysis by a filter-membrane peel technique: *Amer. Mineral.* **58**, 553–554.
- Eggleton, R. A. and Buseck, P. R. (1980) High resolution electron microscopy of feldspar weathering: *Clays & Clay Minerals* **28**, 173–178.
- Howard, J. J. (1981) Lithium and potassium saturation of illite/smectite clays from interlaminated shales and sandstones: *Clays & Clay Minerals* **29**, 136–142.
- Hower, J., Eslinger, E. V., Hower, M., and Perry, E. A. (1976) Mechanism of burial metamorphism of argillaceous sediment: 1. Mineralogy and chemical evidence: *Geol. Soc. Amer. Bull.* **87**, 725–737.
- Lagaly, G. (1982) Layer charge heterogeneity in vermiculites: *Clays & Clay Minerals* **30**, 215–222.
- Lagaly, G. and Weiss, A. (1969) Determination of the layer charge in mica-type layer silicates: in *Proc. Int. Clay Conf., Tokyo, 1969, Vol. 1*, L. Heller, ed., Israel Univ. Press, Jerusalem, 61–80.
- Lee, S. Y., Jackson, M. L., and Brown, J. L. (1975) Micaeous occlusion in kaolinite observed by ultramicrotomy and high resolution electron microscopy: *Clays & Clay Minerals* **23**, 125–129.
- Nadeau, P. H., Tait, J. M., McHardy, W. J., and Wilson, M. J. (1984a) Interstratified XRD characteristics of physical mixtures of elementary clay particles: *Clay Miner.* **19**, 67–76.
- Nadeau, P. H., Wilson, M. J., McHardy, W. J., and Tait, J. M. (1984b) Interparticle diffraction: a new concept for interstratified clays: *Clay Miner.* **19**, 757–769.
- Page, R. and Wenk, H. R. (1979) Phyllosilicate alteration of plagioclase studied by transmission electron microscopy: *Geology* **7**, 393–397.
- Perry, E. A. and Hower, J. (1970) Burial diagenesis in Gulf Coast pelitic sediments: *Clays & Clay Minerals* **18**, 165–177.
- Reynolds, R. C. (1968) The effect of particle size on apparent lattice spacings: *Acta Crystallogr.* **24**, 319–320.
- Reynolds, R. C. (1980) Interstratified clay minerals: in *Crystal Structures of Clay Minerals and Their X-Ray Identification*, G. W. Brindley and G. Brown, eds., Mineralogical Society, London, 305–360.
- Reynolds, R. C. and Hower, J. (1970) The nature of interlayering in mixed-layer illite-montmorillonites: *Clays & Clay Minerals* **18**, 25–36.
- Sawhney, B. L. (1972) Selective sorption and fixation of cations by clay minerals: a review: *Clays & Clay Minerals* **20**, 93–100.

(Received 6 February 1985; accepted 13 July 1985; Ms. 1454)